RESISTANCE OF COIL

The resistance R_{TC} in the RLC model is an effective or equivalent resistance which represents all the losses in the Tesla coil. It includes

1. Ohmic or copper losses
2. Dielectric losses, coil form and conductor insulation
3. Eddy current losses in toroid, strike ring, and soil
4. Radiation losses
5. Losses in the spark

It is surprising how difficult it is to calculate these various losses. Making meaningful measurements can also be challenging. If we operate at low input voltage so we are below spark breakout, then we can ignore the last term for the moment. I will ramble through some considerations for the other losses.

1 Temperature Effects

Almost all coils are wound with copper wire. It is moderately priced and widely available. There might be an occasional aluminum coil, usually from some 'bargain' at a surplus auction. Aluminum has higher resistivity than copper, so to get a given resistance the wire must be physically larger. We saw earlier that to get a high toroid voltage we needed a coil with large L and/or small R. If we use larger wire to keep the resistance the same, the coil must be physically larger and the inductance will decrease. We would expect therefore that aluminum coils would always be inferior to copper coils.

Example

You are given a choice between two spools of magnet wire, each 1000 feet in length. The copper is 24 gauge, with nominal resistance 25.67 Ω, while the aluminum is 22 gauge, with nominal resistance 26.46 Ω. You have a piece of 5 inch diameter PVC pipe and are considering using the entire 1000 ft to wind a coil. You wish to compare the inductances of the two prospective coils.

You assume a build (thickness of dielectric) of 1.65 mils. The diameter of the 22 gauge wire is then $23.35 + 2(1.65) = 28.65$ mils and the diameter of the 24 gauge wire is $20.1 + 2(1.65) = 23.4$ mils. The nominal number of turns would be

$$N = \frac{1000}{\pi(5/12)} = 764$$

The winding length for the 22 gauge wire would be

$$\ell_w = 764(28.65) = 21,890 \text{ mils} = 21.89 \text{ inches}$$

and 17.19 inches for the 24 gauge wire.

By Wheeler's formula, the inductance for the 22 gauge coil would be

$$L = \frac{r^2 N^2}{9r + 10\ell_w} = \frac{(2.5)^2(764)^2}{9(2.5) + 10(21.89)} = 15,110 \;\; \mu\text{H}$$

The 24 gauge coil has an inductance of 18,120 μH. For this particular example where r and N are held fixed, ℓ_w is proportional to wire diameter and since it appears in the denominator, a smaller wire diameter results in a larger inductance.

If we hold the winding length fixed, say at 17.88 inches, then the 1000 ft of aluminum wire will fit on a coil of 624 turns and 6.121 inches diameter. The inductance is now 17,670 μH, larger but still less than that of the copper coil. The aluminum coil has more resistance and less inductance than the copper coil, both undesirable. As a side issue, if we hold the winding length fixed, the coil gets to be relatively short and fat. Standard wisdom is that the ratio of length to diameter needs to be on the order of four or five, so this is another negative factor. You should buy the copper wire.

Aluminum forms a coating of aluminum oxide when exposed to air. This oxide is not a conductor (copper oxide is) so there is always a problem in making electrically solid connections. This is not an unsolvable problem since electric utilities use aluminum wire almost exclusively, for cost and weight reasons. The trained individual with the right tools might be able to get acceptable performance from an aluminum coil. The rest of us should stick with copper.

Silver is slightly more conductive than copper, but the price is much higher. Copper losses are not considered that big a factor in coil performance, so there is little incentive to go to silver wire.

The dc resistance of copper wire is determined by table look-up or by measurement with an ohmmeter. The tables typically give the resistance of 1000 ft of wire at a specified temperature, say 20^{o}C or 68^{o}F. The tables give the resistance to four significant places, but using more than three is somewhat of a joke because of the resistance variation with temperature. If the table resistance is R_1 at a temperature T_1, then the resistance R_2 at some other temperature T_2 is

$$R_2 = R_1 \frac{T_2 - T_i}{T_1 - T_i} \tag{1}$$

where T_i is the *inferred absolute zero temperature*, -234.5^oC for copper. If the table resistance is given for 20^{o}C, then the resistance of a copper wire at temperature T_2 is

$$R_2 = R_1 \frac{T_2 + 234.5}{20 + 234.5} \tag{2}$$

The resistance has dropped to 90% of the tabulated value at -5.45^oC (not impossible for an unheated shop in some parts of the world) and is at 110% of the tabulated value at 45.45^oC. The wire could certainly rise to this temperature during operation even on a pleasant day.

The inferred absolute zero temperature does not have much to do with absolute zero (-273^oC). Pure iron has an inferred absolute zero of -162^oC and Manganin has an inferred absolute zero of $-167,000^o$C. The fact that the inferred absolute zero of copper is not drastically different from absolute zero makes it useful as a temperature sensor. If one is curious about how warm a Tesla coil got during operation, the best way of measuring the temperature is to measure the dc resistance and work backwards through the above equations.

2 Skin Effect

At dc, current flows uniformly across the entire cross section of the conductor. As frequency increases, however, a phenomenon called skin effect causes less of the total current to flow in the center of the wire. Having less conductor available causes the resistance to increase.

An expression for skin depth can be derived as

$$\delta = \frac{1}{\sqrt{\pi f \mu \sigma}} \tag{3}$$

where f is the frequency in Hz, μ is the permeability of the conductor ($4\pi \times 10^{-7}$ for nonferromagnetic materials), and σ is the conductivity.

The skin depth for copper at 20^oC is

$$\delta = \frac{0.066}{\sqrt{f}} \quad \text{m} \tag{4}$$

Most introductory electromagnetic theory books derive the expression for ac resistance as

$$R_{ac} = R_{dc}\frac{b}{2\delta} \tag{5}$$

where b is the radius of the wire and δ is the skin depth, in consistent units. This equation is only valid for $\delta \ll b$. As might be expected, this excludes most Tesla coils, so we must find other expressions.

A number of more advanced electromagnetic theory books derive an expression for the ac resistance. Typical is the treatment by Ramo, Whinnery, and Van Duzer [6]. They start with Maxwell's Equations, and write a differential equation for the current density $J_z(r)$ inside an isolated straight cylindrical conductor centered on the z axis.

$$\frac{d^2J_z}{dr^2} + \frac{1}{r}\frac{dJ_z}{dr} + T^2J_z = 0 \tag{6}$$

where

$$T^2 = -j\omega\mu\sigma = -j(2\pi f\mu\sigma) = -j\frac{2}{\delta^2} \tag{7}$$

The solution for current density is

$$J_z = AJ_0(Tr) \tag{8}$$

where $J_0(Tr)$ is the Bessel function of the first kind and zero order.

The infinite series for this Bessel function is

$$J_0(Tr) = \sum_{m=0}^{\infty} \frac{(-1)^m \left(\frac{Tr}{2}\right)^{2m}}{(m!)^2} = \sum_{m=0}^{\infty} \frac{(-1)^m (T^2)^m r^{2m}}{2^{2m}(m!)^2} \tag{9}$$

When we insert the above expression for T^2, the series becomes

$$J_0(Tr) = \sum_{m=0}^{\infty} \frac{(-1)^m(-j)^m \left(\frac{2}{\delta^2}\right)^m r^{2m}}{2^{2m}(m!)^2} \tag{10}$$

Note that

$$(-1)^m(-j)^m = (j)^m \tag{11}$$

$$\frac{2^m}{2^{2m}} = \frac{1}{2^m} \tag{12}$$

$$\frac{r^{2m}}{\delta^{2m}} = \left(\frac{r}{\delta}\right)^{2m} \tag{13}$$

With these substitutions, we can write

$$J_0(Tr) = \sum_{m=0}^{\infty} \frac{(j)^m \left(\frac{r}{\delta}\right)^{2m}}{2^m(m!)^2} \tag{14}$$

The series can now be split into its real and imaginary parts.

$$\text{Real}[J_0(Tr)] = 1 - \frac{\left(\frac{r}{\delta}\right)^4}{2^2(2!)^2} + \frac{\left(\frac{r}{\delta}\right)^8}{2^4(4!)^2} - + \cdots \tag{15}$$

$$\text{Imag}[J_0(Tr)] = \frac{\left(\frac{r}{\delta}\right)^2}{2(1!)^2} - \frac{\left(\frac{r}{\delta}\right)^6}{2^3(3!)^2} + \frac{\left(\frac{r}{\delta}\right)^{10}}{2^5(5!)^2} - + \cdots \tag{16}$$

These are related to the ber and bei functions as follows.

$$\text{Real}[J_0(Tr)] = \text{ber}(\sqrt{2}r/\delta) \tag{17}$$

$$\text{Imag}[J_0(Tr)] = \text{bei}(\sqrt{2}r/\delta) \tag{18}$$

There are several ways to proceed to find the ac resistance. One is to use one of Maxwell's curl equations to find the magnetic field inside the wire, a constant times the derivative of the electric field. This magnetic field is used to find the total current in the wire. The electric field times the wire length ℓ is the total voltage. The ac resistance is just the real part of the ratio of voltage to current.

To my knowledge, every method of finding the ac resistance is tedious. I will proceed with a basic Circuit Theory I type approach. Consider the straight wire as formed of N concentric cylinders, as shown in Fig. 1.

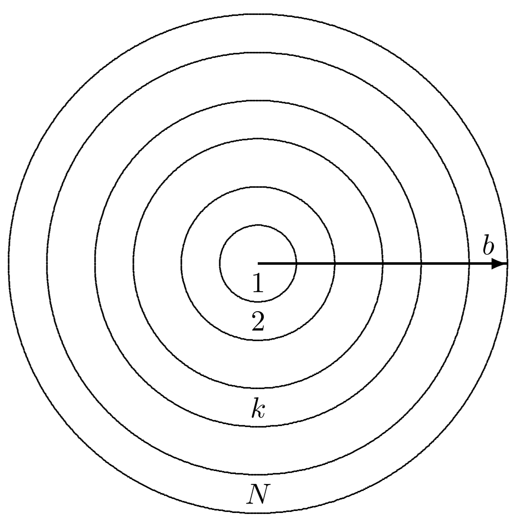

Figure 1: Wire Formed of Concentric Cylinders

The wire radius is b. The radius to each boundary between cylinders is designated by r_k, where $r_N = b$, $r_1 = b/N$, $r_0 = 0$, etc. The cross sectional area of cylindrical shell k is

$$\text{Area} = \pi(r_k^2 - r_{k-1}^2) \tag{19}$$

The dc resistance of cylindrical shell k is

$$R_{dck} = \frac{\rho\ell}{\pi(r_k^2 - r_{k-1}^2)} \tag{20}$$

where ρ is the resistivity and ℓ is the length of the wire. The dc resistance of the entire wire is

$$R_{dc} = \frac{\rho\ell}{\pi b^2} \tag{21}$$

The average current density in a shell is approximately the current density at the midpoint of a shell. That is,

$$J_{zk} = AJ_0(Tr) \qquad \text{for } r = \frac{r_k + r_{k-1}}{2} \tag{22}$$

The current in shell k is

$$I_k = J_{zk}\pi(r_k^2 - r_{k-1}^2) \tag{23}$$

Note that I_k is a phasor. Both the magnitude and the phase of the current and current density vary from the center to the surface of the wire.

The total current is given by

$$I = \sum_{k=1}^{N} I_k \tag{24}$$

where all the real parts of the various I_k are added together, and all the imaginary parts, to form the phasor I. The power dissipated in shell k is

$$P_k = I_k I_k^* R_{dck} \tag{25}$$

where $I_k I_k^*$ indicates that the current has been multiplied by its complex conjugate to form $|I_k|^2$. The total power dissipated in the wire is

$$P = \sum_{k=1}^{N} P_k \tag{26}$$

But by definition

$$P = |I|^2 R_{ac} \tag{27}$$

Therefore,

$$R_{ac} = \frac{P}{|I|^2} = \frac{\sum_{k=1}^{N} P_k}{|I|^2} \tag{28}$$

and

$$\frac{R_{ac}}{R_{dc}} = \frac{\sum_{k=1}^{N} P_k}{R_{dc}|I|^2} \tag{29}$$

We need to do one more step to get this formula into computational form. The ratio of resistances is independent of a specific current flow so we can set $A = 1$ in Eq. 22. For shorthand we will write the real part of J_{zk} as $\text{RE}J_k$ and the imaginary part as $\text{IM}J_k$. After pages of algebra, all the terms like $\rho\ell$ cancel out and we have the final result.

$$\frac{R_{ac}}{R_{dc}} = \frac{\sum_{k=1}^{N}[\text{RE}J_k^2 + \text{IM}J_k^2]\left(\left(\frac{r_k}{b}\right)^2 - \left(\frac{r_{k-1}}{b}\right)^2\right)}{\left[\sum_{k=1}^{N}\text{RE}J_k\left(\left(\frac{r_k}{b}\right)^2 - \left(\frac{r_{k-1}}{b}\right)^2\right)\right]^2 + \left[\sum_{k=1}^{N}\text{IM}J_k\left(\left(\frac{r_k}{b}\right)^2 - \left(\frac{r_{k-1}}{b}\right)^2\right)\right]^2} \tag{30}$$

The algebra basically normalizes itself to use a cylinder of unit radius. The variable is skin depth, which appears in the argument of the Bessel function as r/δ. If the wire radius is one skin depth, the ratio $R_{ac}/R_{dc} = 1.020$, so the dc resistance can be used for any wire for which the radius is less than a skin depth. Other values are given in Table 1.

Table 1: R_{ac}/R_{dc} for various values of b/δ.

b/δ	R_{ac}/R_{dc}
1	1.020
2	1.263
3	1.763
4	2.261
5	2.743
6	3.221
7	3.693
8	4.154

This analytic technique of finding the ac resistance has been around for a long time and is described in many books. Before the advent of computers, it was difficult to use. One would use tables of Bessel functions which listed real and imaginary components separately, such as Jahnke and Emde [4]. The notation among different authors differed, making it difficult to compare results. Of course, computers have now made the task of calculating these infinite series much more manageable. Actually, if the wire radius is not more than about 8 skin depths, the first 12 terms of Eq. 14 are more than adequate.

Because of the difficulties of using this analytic technique before computers, people developed lookup tables and empirical models to find R_{ac}/R_{dc}. For historical interest and for the benefit of any reader adverse to writing computer code, we will present the approximations developed by Terman [8], who has a detailed discussion of this topic. He defines R_{ac} in terms of a parameter x, where

$$x = \pi d \sqrt{\frac{2f}{\rho(10^7)}} \tag{31}$$

for nonmagnetic materials. Here, d is the conductor diameter in meters, f is the frequency in Hz, and ρ is the resistivity in ohm meters. As x gets very small, due to either low frequency or small wire, the ac resistance approaches the dc resistance. Above about $x = 3$, R_{ac}/R_{dc} varies essentially linearly with x according to the expression

$$\frac{R_{ac}}{R_{dc}} = 0.3535x + 0.264 \qquad (x > 3) \tag{32}$$

Terman gives the following tabular values of R_{ac}/R_{dc} for x between 0 and 3.

Table 2: R_{ac}/R_{dc} for various values of x.

x	R_{ac}/R_{dc}	x	R_{ac}/R_{dc}
0	1.0000	1.5	1.026
0.5	1.0003	1.6	1.033
0.6	1.0007	1.7	1.042
0.7	1.0012	1.8	1.052
0.8	1.0021	1.9	1.064
0.9	1.0034	2.0	1.078
1.0	1.005	2.2	1.111
1.1	1.008	2.4	1.152
1.2	1.011	2.6	1.201
1.3	1.015	2.8	1.256
1.5	1.020	3.0	1.318

For copper, $\rho = 1.724 \times 10^{-8}$ ohm meters. For those of us still using wire tables in English units, where wire diameters are given in mils (1 mil = 0.001 inch), Terman [8] has reduced the expression for x to

$$x = 0.271 d_m \sqrt{f_{MHz}} \tag{33}$$

where d_m is the wire diameter in mils and f_{MHz} is the frequency in MHz.

For example, the 14 ga coil being examined here has a dc resistance of 3.99 Ω at 20^{o}C. For a large toroid, the resonant frequency is 160 kHz. The nominal diameter of 14 ga wire is 64.08 mils. We calculate x as

$$x = 0.271(64.08)\sqrt{0.16} = 6.946$$

The ac resistance of the wire in the coil (assuming the wire is uncoiled and is supported in one straight line) is then

$$R_{ac} = 3.99(0.3535(6.964) + 0.264) = 10.85 \quad \Omega$$

We see that skin effect makes a significant difference in resistance, especially where larger wire sizes or higher frequencies are used.

The two methods presented here (Terman and the one using Bessel functions) should yield very nearly the same results if we use the relationship

$$x = 1.412 \frac{b}{\delta} \tag{34}$$

For example, if $b/\delta = 3$, then $x = 4.236$ and

$$\frac{R_{ac}}{R_{dc}} = 0.3535(4.236) + 0.264 = 1.761 \tag{35}$$

which is reasonably close to the value of 1.763 given in Table 1.

3 Proximity Effect

The effect of adjacent turns in the coil causes the current density to be even more nonuniform than for the straight wire, which raises the resistance even more. This effect is called the *proximity effect*. Terman [8] has a curve for two straight parallel cylinders carrying current the same direction that shows an increase of about 33% for the wires touching physically (but not electrically), and an increase of about 10% for the case when the two wires are separated by a gap equal to the wire diameter.

Medhurst

But our problem is not that of two parallel wires going to infinity, but that of hundreds of turns of wire in a finite space. Perhaps the first person to examine this problem experimentally was Medhurst [5]. We saw his results for the self-capacitance of a coil back in Chapter 2. The same paper gives tables for ϕ_M, the increase in resistance over R_{ac} as a function of coil length over coil diameter and wire diameter over wire spacing. Since such tests are critical to our Tesla coil model, it seems appropriate to discuss his paper in some detail.

Medhurst used between 30 and 50 turns of bare copper wire wound in grooves of a low loss dielectric former. The former material was Distrene, which he claimed to have a power factor of about 0.0003. The coil and former were dried carefully before testing. This means that dielectric losses in the coil form, winding insulation, and humidity should be negligible. He did not mention the possibility of eddy current losses, but I suspect these were negligible as well. Testing was done at low power, so corona or spark losses would have been zero. His test method did not separate ohmic (heating) losses from radiation losses. Standard wisdom is that radiation from small coils at relatively low frequencies is negligible, and I have seen no contrary evidence, so it will be assumed that his results apply to ohmic heating.

He used two different wire sizes, 18 and 20 s.w.g. I assume these refer to the British Standard Wire Gauge, where 18 s.w.g. has a diameter of 48 mils (1.219 mm) and 20 s.w.g. has a diameter of 36 mils (0.9144 mm). For the tight wound case, he used double-silk-covered (dsc) or single-silk-covered conductors. Such coatings are not readily available today, so it would be hard to replicate his findings.

A confusing aspect of his paper is that the symbol H is used in four different ways. It is used for magnetic field and for the unit of inductance, both of which are immediately obvious and not a problem. It is used for a function of coil length over coil diameter as we saw in Chapter 2, where $C_M = HD$ for the self-capacitance (or Medhurst capacitance) of a coil. Then the symbol is also used for a function of wire diameter and skin depth in determining the ac resistance. Some other symbol would have been more appropriate.

The coils Medhurst tested are not 'typical' Tesla coils. Tesla coils usually have far more than his 30 - 50 turns. He tested at frequencies of around 1 MHz, somewhat above most Tesla coil operating frequencies. He restricted himself to cases where the skin depth is a small fraction of the wire diameter.

We might define a Medhurst resistance R_M, similar to the Medhurst capacitance C_M, where

$$R_M = R_{ac}(1 + k_f(\phi_M - 1)) \tag{36}$$

where k_f is a monotonic function of frequency that is zero for very low frequencies and unity for very high frequencies. That is,

$$R_M = \phi_M R_{ac} \qquad f \text{ large} \tag{37}$$

and

$$R_M = R_{ac} \approx R_{dc} \qquad f \text{ small} \tag{38}$$

Medhurst makes no attempt to find k_f. Therefore we will have to restrict ourselves to the case of high frequencies, where the proximity effect is fully 'saturated', or where the wire radius is several skin depths thick. ϕ_M is given in his Table VIII. A portion of that table is shown in Table 3.

Table 3: Experimental values of ϕ_M, the ratio of high-frequency coil resistance to the resistance at the same frequency of the same length of straight wire.

	ℓ_w/D						
d/z_1	1	2	4	6	8	10	∞
1	5.55	4.10	3.54	3.31	3.20	3.23	3.41
0.9	4.10	3.36	3.05	2.92	2.90	2.93	3.11
0.8	3.17	2.74	2.60	2.60	2.62	2.65	2.81
0.7	2.47	2.32	2.27	2.29	2.34	2.37	2.51
0.6	1.94	1.98	2.01	2.03	2.08	2.10	2.22
0.5	1.67	1.74	1.78	1.80	1.81	1.83	1.93
0.4	1.45	1.50	1.54	1.56	1.57	1.58	1.65
0.3	1.24	1.28	1.32	1.34	1.34	1.35	1.40

In this table, ℓ_w is the coil winding length, D is the coil diameter, d is the diameter of the copper wire, and z_1 is the center-to-center spacing between adjacent turns, all in consistent units.

This table indicates that the proximity effect can easily double or triple the measured input resistance over that predicted by R_{ac} for a straight wire of the same length. In the previous subsection, a 14 gauge coil was mentioned which had a dc resistance of 3.99 Ω, and an ac resistance of 10.85 Ω at 160 kHz. By interpolation in Table 3, ϕ_M is found to be 1.85. Therefore, the predicted ohmic resistance of the coil would be (1.85)(10.85) = 20 Ω (at sufficiently high frequencies). The measured input resistance is about 23 Ω at resonance. This measured resistance includes dielectric losses and eddy current losses in addition to ohmic losses. The difference of 3 Ω would represent eddy current, dielectric, and transmission line losses, which is probably not far from reality. If the proximity effect is not fully 'saturated', the predicted resistance would be less, and the difference between predicted and measured would be greater.

Poynting

I then started thinking about methods to explain and perhaps even calculate ϕ_M. Note that we are still operating in the circuit theory mode here, such that the current is the same in every turn of the coil. The effect of distributed capacitance, which causes the current to be different in different turns will be discussed later. I worked on two different methods that I had not seen in the literature. One was to use Poynting's vector and calculate power flow into the copper of the coil from the total magnetic and electric fields. The other was to split the current into filaments and require a distribution of filament currents that would minimize the magnetic field in the center of the wire. Both methods worked to some degree if ℓ_w/D was not too short. After discussing these two methods, I will present some results from a recent paper [2]. This paper is computationally superior to my two methods, but still is not all that great for short coils. I have come to realize that finding the resistance of a short coil is a tough problem. I am tempted to take up golf or something less frustrating!

The Poynting vector is defined as

$$\mathbf{S} = \mathbf{E} \times \mathbf{H} \quad \mathrm{W/m^2} \tag{39}$$

where $\times$ refers to the cross product of two vectors.

A student in Circuit Theory I will hear the instructor say that power flows down a wire *inside* the wire (electrons bumping along). The student will walk next door and hear the EM Theory instructor say that *obviously* power flows down the *outside* of a wire in the form of electric and magnetic fields. The speed of propagation is determined by the dielectric constant of the insulating material, not by any property of the conductor, hence the action must be happening outside the copper. The wire gets hot due to some leakage of the fields from outside to inside through the mechanism of Poynting's vector.

Most students compartmentalize this information, so think power flows one place in one class and the opposite place in another class, and rarely ask where the power really flows. The problem is that no one really knows. Correct answers are obtained with either approach.

There is a problem, in that Poynting's vector does not appear to work in some cases. Consider the following example.

Example

On a clear day the average electric field is 130 V/m at the surface of the earth, directed down (the earth is negatively charged with respect to space). At the earth's magnetic equator, the earth's magnetic flux density $B = \mu H$ is horizontal, with magnitude about half a gauss, or 0.5×10^{-4} T. If **E** is directed 'down' and **H** is directed 'south', then the Poynting vector **S** is directed 'west'. The magnitude is

$$S = EH = \frac{EB}{\mu_o} = \frac{130(0.5 \times 10^{-4})}{4\pi \times 10^{-7}} = 5200 \quad \mathrm{W/m^2}$$

A power density of 5200 W/m^2 would be very noticeable, but our senses tell us that nothing is actually flowing. No one has built a machine to extract and sell this power. A student who asks about this problem is likely to get one of two responses. The first is a raised voice and some subtle ridicule for asking such a dumb question. The second is a variant of "Trust me. Sometimes the electron acts like a wave, sometimes like a particle. We who have already been initiated into the scientific priesthood will train you to know when it acts like what." But I digress.

Standard wisdom among the priesthood is that Poynting's vector works when **E** and **H** are the cause and effect of each other, or are both produced by the same source. If current is flowing in a wire, it produces a magnetic field around the wire and a voltage drop (electric field) along the wire, so this is a proper application.

For a straight conductor centered on the z axis, the magnetic field **H** is given by

$$\mathbf{H} = \frac{I}{2\pi r}\mathbf{a}_\phi \tag{40}$$

where I is the current flowing in the conductor, r is the distance from the z axis, and $\mathbf{a}_\phi$ is the unit vector in the ϕ direction around the conductor. The current I produces a voltage drop along the conductor and the electric field is $\mathbf{E} = IR'\mathbf{a}_z$ where R' is the resistance per unit length. The cross product $\mathbf{a}_z \times \mathbf{a}_\phi = -\mathbf{a}_r$, so the Poynting vector is directed into the conductor.

The magnitude of the Poynting vector entering a straight wire of radius b is

$$S_b = EH = IR'\frac{I}{2\pi b} \tag{41}$$

The total power entering the conductor is determined by integrating the Poynting vector over its surface. If the wire length is ℓ and the radius is b, the power is

$$P_b = \int_0^{2\pi}\int_0^{\ell}(IR')(\frac{I}{2\pi b})b\,d\phi\,dz = I^2R'\ell \tag{42}$$

which is exactly what is predicted by standard circuit theory.

The magnetic field of a filamentary loop, carrying a current I, centered on the z axis and located in the xy plane is [7]

$$H_\rho = \frac{I}{2\pi}\frac{z}{\rho\sqrt{(a+\rho)^2+z^2}}\left[-K + \frac{a^2+\rho^2+z^2}{(a-\rho)^2+z^2}E\right] \tag{43}$$

$$H_z = \frac{I}{2\pi}\frac{1}{\sqrt{(a+\rho)^2+z^2}}\left[K + \frac{a^2-\rho^2-z^2}{(a-\rho)^2+z^2}E\right] \tag{44}$$

where K and E are the complete elliptic integrals of the first and second kind. The general structure is shown in Fig. 2, which shows three turns out of an N-turn Tesla coil. Coil diameter is D and the radius of the individual wires is b. The distance between adjacent turns is z_1 and the overall winding length is ℓ_w. Current is flowing into the paper on the right, and out of the paper on the left. The electric field in each conductor is in the same direction as the current.

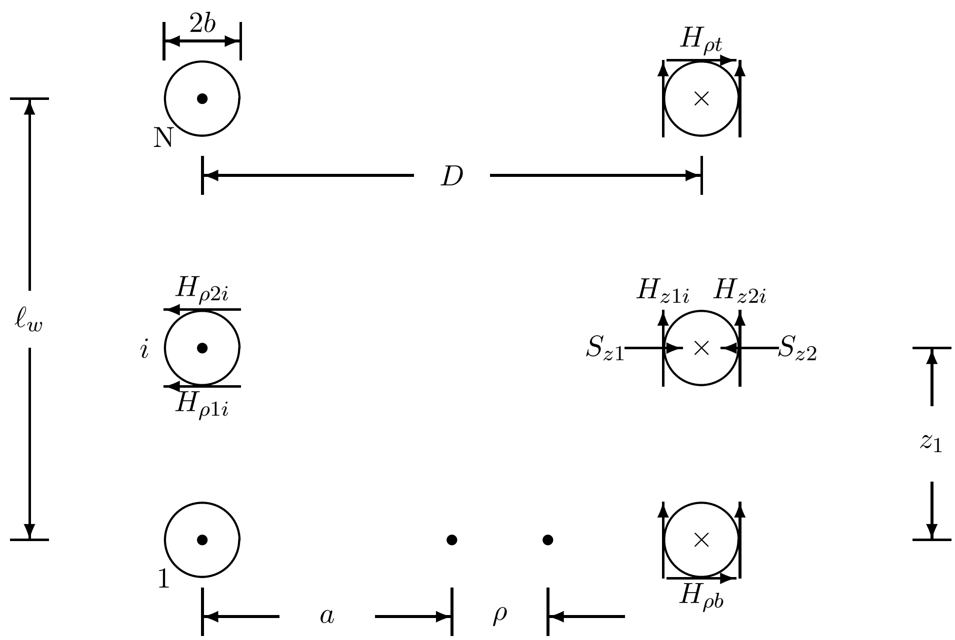

Figure 2: Three Turns of Tesla Coil

The elliptic integrals K and E are functions of a parameter k, where

$$k^2 = \frac{4a\rho}{(a+\rho)^2 + z^2} \tag{45}$$

One can either look up the values for K and E in a math table, or can evaluate their infinite series representation. The series converges relatively slowly, so computation of the first one or two thousand terms is not unreasonable, using double precision numbers.

As might be expected, people have developed techniques for calculating these elliptic integrals with less computational effort. Gauss's method using the arithmetic-geometric mean method converges very fast, usually in less than 20 terms for 10-digit accuracy [1] . The incremental H field on the inside surface of turn i that is produced by current I in turn j is given by

$$\Delta H_{z1i} = \frac{I}{2\pi}\frac{1}{\sqrt{(2a-b)^2 + (i-j)^2 z_1^2}}\left[K + \frac{a^2 - (a-b)^2 - (i-j)^2 z_1^2}{b^2 + (i-j)^2 z_1^2}E\right] \tag{46}$$

and similarly for the field on the outside of the coil, ΔH_{z2i}. The total field H_{z1i} is found by summation.

$$H_{z1i} = \sum_{j=1}^{N} \Delta H_{z1i} \tag{47}$$

Similar expressions hold for H_{z2i}, $H_{\rho 1i}$, and $H_{\rho 2i}$. These four fields are tabulated in Table 4 for a 21 turn coil with $\ell_w/D = 1$ and $2b = z_1$. This corresponds to the upper left corner of Table 3.

Table 4: Predicted values of H_{z1i}, H_{z2i}, $H_{\rho 1i}$, and $H_{\rho 2i}$ in A/m for a 21 turn coil with $\ell_w/D = 1$ and $d/z_1 = 1$. $D = 8$ inches and $d = 2b = 0.4$ inches.

i	H_{z1i}	H_{z2i}	$H_{\rho 1i}$	$H_{\rho 2i}$
1	65.16	-19.79	-66.47	-35.09
2	73.92	-23.69	-35.09	-24.72
3	77.62	-23.76	-24.72	-18.60
4	79.92	-23.19	-18.60	-14.32
5	81.58	-22.52	-14.32	-11.06
6	82.82	-21.90	-11.06	-8.42
7	83.76	-21.36	-8.42	-6.20
8	84.46	-20.94	-6.20	-4.26
9	84.93	-20.64	-4.26	-2.49
10	85.21	-20.46	-2.49	-0.82
11	85.31	-20.40	-0.82	0.82
12	85.21	-20.46	0.82	2.49
13	84.93	-20.64	2.49	4.26
14	84.46	-20.94	4.26	6.20
15	83.76	-21.36	6.20	8.42
16	82.82	-21.90	8.42	11.06
17	81.58	-22.52	11.06	14.32
18	79.92	-23.19	14.32	18.60
19	77.62	-23.76	18.60	24.72
20	73.92	-23.69	24.72	35.09
21	65.16	-19.79	35.09	66.47

We see that the magnetic field is up on the inside of the coil and down on the outside. Likewise, it is directed radially inward over the bottom half of the coil (turns 1-10) and outward over the top half of the coil. The z component is largest in the middle of the coil, while the ρ component is largest at the ends.

The total power flowing into the hollow cylinder bounding the coil is then

$$\begin{aligned} P &= \int S\, d(\text{area}) \approx (\text{Area})(E)(\sum H) \\ &= \ell_t 2b(IR')(H_{\rho t} - H_{\rho b}) + \ell_t z_1 (IR')(\sum_{i=1}^{N}(H_{z1i} - H_{z2i})) \end{aligned} \tag{48}$$

(49)

where ℓ_t is the length of one turn and I have added the magnetic fields $H_{\rho t}$ and $H_{\rho b}$ to include the end effects at the top and bottom of the coil. The minus sign in front of the H_{z2i} term is necessary to indicate that the Poynting vector is into the copper on the outside of the coil as well as on the inside, and likewise for the $H_{\rho b}$ term.

The power flowing into the same length of straight wire would be

$$P_{st} = (\text{Area})(E)(H) = (N)(\ell_t)(2\pi b)(IR')(\frac{I}{2\pi b}) \tag{50}$$

Power is proportional to resistance so the ratio of P to P_{st} is another ϕ, call it ϕ_p to distinguish it from the Medhurst ϕ. The ϕ_p is

$$\phi_p = \frac{\ell_t 2b(IR')(H_{\rho t} - H_{\rho b}) + \ell_t z_1 (IR')(\sum_{i=1}^{N}(H_{z1i} - H_{z2i}))}{N\ell_t 2\pi b IR'(I/2\pi b)} \tag{51}$$

Canceling the common terms gives

$$\phi_p = \frac{H_{\rho t} - H_{\rho b} + \sum_{i=1}^{N}(H_{z1i} - H_{z2i})}{1/2\pi b} \tag{52}$$

For the case shown in Table 4,

$$\phi_p = \frac{2273.92}{(21)(31.33)} = 3.456 \tag{53}$$

We see that this approach yields an increase in resistance of the coil as compared with the same amount of straight wire of 3.456, as compared with the Medhurst prediction of 5.55. This is within a factor of two, as mentioned earlier, but is not really close enough for any definitive computations. After spending considerable time looking at the problem, I decided that one significant flaw in the analysis is that it assumes the actual current flow throughout the conductor cross section can be modeled by a filamentary current (of the same total magnitude) flowing exactly in the center of each conductor. The actual current density is higher near the surface of the conductor due to skin effect, but will not be symmetric inside to outside, or top to bottom, hence the equivalent current filament will not be in the exact center. The computations are sensitive to the position or location of the current, and if this is not accurately known, it will not be possible to obtain highly accurate results with this Poynting vector approach.

Boundary Conditions

My next analytic attempt was to split the current flow into four filaments, located on the surface at the top, bottom, inside, and outside of each turn. The magnetic field components H_z and H_ρ were calculated at the center of the wire cross section, using Eqns. 43 and 44. The computations are very similar to those of the previous Poynting vector effort. Instead of finding the fields on the wire surface from a current at the wire center, I find the fields at the wire center from current filaments on the surface.

In the high frequency limit, the magnetic field at the center of a conductor will be zero. Currents will distribute themselves to meet this boundary condition. The problem then becomes one of iteration to find a current distribution that will cause the magnetic field to be zero at the center of the conductor. For example, suppose we start with a total current flow of 4 A, or four filaments each carrying 1 A. We calculate the sum of H_z and H_ρ at the center of each turn. We then move a portion of the current in one filament, say 0.1 A, to another filament, and recalculate the sum of the fields. If the sum is smaller, we are headed the right direction, and try moving some more current from the first filament to the second. When we reach the zero field condition, we have found a solution to Maxwell's Equations.

One obvious problem with this simple algorithm is that the limit is found when all the current flows in one filament. If we think of the wire as four quadrants in parallel, but no current is flowing in three of the quadrants, it is like removing three out of four parallel resistors. The resistance of one quadrant is four times the resistance of the entire wire. This approach will yield a maximum ϕ_M of 4.00, not the 5.55 appearing in the upper left corner of Table 3. One can get past this limit by splitting the conductor into more than four filaments, say 8 or 16, or by allowing negative current in some of the filaments.

I tried 8 filaments, but this did not immediately fix the problem. It did not appear to be possible to get to the case of zero magnetic field in the center of the wire while requiring all currents to be non negative. If we allow currents to be negative, such that current is flowing in one direction on one side of the conductor and in the opposite direction on the other side, there must be some lateral or azimuthal flow of current. This violates our original assumption of current flowing only in the direction of the conductors. My mother told me there would be days like this!

While this is certainly an interesting problem in its own right, it has only limited application to Tesla coils which usually have a length/diameter ratio on the order of four. The maximum ϕ_M is now 3.54, from Table 3, which can be analyzed with four filaments and non negative currents. Results of the analysis are shown in Table 5. The column labeled ϕ_M is from Table 3 while the column labeled ϕ_J is for the predicted resistance ratio from this iterated computer program.

Table 5: Comparison of ϕ_M with ϕ_J for a coil with $\ell_w/D = 4$

d/z_1	ϕ_M	ϕ_J
1.0	3.54	3.36
0.9	3.05	3.11
0.8	2.60	2.63
0.7	2.27	2.30
0.6	2.01	1.99
0.5	1.78	1.80
0.4	1.54	1.60
0.3	1.32	1.40

It can be seen that agreement is quite good between the Medhurst measured values and the calculated values using the four-filament approach. I feel that the Medhurst table has been theoretically validated. I am sure that there are other methods of theoretically determining ϕ_M, perhaps easier and more accurate, but this approach convinced me that proximity effect does indeed have a classical explanation, if one wants to spend the time and effort necessary to find it. In the meantime, Table 3 should be quite adequate for anyone looking for an estimate of the high frequency resistance of a coil of wire.

Fraga

After preparing the above material, a reviewer [1] informed me of a paper by Fraga, Prados, and Chen on this topic [2]. An examination of the paper indicated that the authors seemed to be restricting themselves to the following case.

1. *Long* solenoids
2. Tight wound solenoids
3. Solenoids with negligible distributed capacitance
4. Low frequency ($b \leq \delta$)
5. Multilayered coils

A typical Tesla coil has a length/diameter ratio of about four (not necessarily *long*). Some coils are space wound. Distributed capacitance is always a problem. It will be discussed in the next section. Tesla coils are usually operated at frequencies where the wire radius will be between one and five skin depths, not less than a single skin depth. And Tesla coils are almost never multilayered. So it was not obvious that the paper would be of much use to the Tesla coil community. On the other hand, Tesla coilers are infamous for using things outside their normal operating range (e.g. pulling 60 mA from a neon sign transformer rated at 30 mA), so I looked some more. The authors have developed a relatively simple closed-form expression for the resistance of a coil, not requiring summations or interpolations, so it would be very nice if it worked for the typical Tesla coil.

Their Eq. 35, expressed in my notation for the single-layer coil is

$$R_s = \frac{2\pi N^2 \rho_{\text{eff}} a[\sinh 2\theta + \sin 2\theta]}{\delta_s \ell_w [\cosh 2\theta - \cos 2\theta]} \tag{54}$$

where N is the number of turns, a is the radius of the coil, and ℓ_w is the winding length of the coil. The other terms are described in the following.

One of the difficulties in the analysis of a coil is that the conductor surfaces are not at a fixed distance from the axis of the coil. A fingernail pressed against the coil moves in and out as the hand moves down the coil. Boundary conditions cannot be simply expressed in this geometry. These authors circumvent this problem by converting round wire to square wire with the same cross-sectional area. They deal with the gap between the wires, due to insulation, by elongating the square conductor toward its neighbor until it touches mechanically (but not electrically). The resistivity is increased a proportional amount such that the resistance remains the same.

Let the radius of a cylindrical wire be b, covered by a dielectric coating of thickness s. Define a square conductor with side y with the same area. Then

$$y^2 = \pi b^2 \tag{55}$$

or

$$y = \sqrt{\pi} b \tag{56}$$

The length of one turn is $2b + 2s$. The effective resistivity for this rectangular wire of thickness y is

$$\rho_{\text{eff}} = \rho \frac{2b + 2s}{y} = \frac{2\rho}{\sqrt{\pi}}(1 + \frac{s}{b}) \tag{57}$$

where ρ is the usual resistivity of the conductor (1.724×10^{-8} ohm meters for copper at 20^{o}C).

They then define an effective skin depth

$$\delta_s = \sqrt{\frac{2\rho_{\text{eff}}}{\mu_0 \omega}} = \sqrt{\frac{4\rho(1 + s/b)}{\sqrt{\pi}\mu_0(2\pi f)}} = \sqrt{\frac{4(1.724 \times 10^{-8}(1 + s/b)}{\sqrt{\pi}(4\pi \times 10^{-7})(2\pi)f}} = 0.0702\sqrt{\frac{1 + s/b}{f}} \tag{58}$$

for copper. The last variable, θ, is then defined as

$$\theta = \frac{y}{\delta_s} = \frac{\sqrt{\pi} b}{\delta_s} \tag{59}$$

One big advantage of this approach is that both the skin depth and the proximity effect are included in one equation that would fit on most programmable calculators. Input quantities are wire radius, coil radius and length, number of turns, and frequency, all readily available. Using the Medhurst approach outlined earlier requires one to first find the ac resistance and then multiply this by a factor ϕ_M found by interpolation in Table 3.

A disadvantage of the Fraga method is that the resistance is equivalent to the last column in Table 3. That is, we find the resistance of a section of an infinitely long coil. This method is not capable of properly dealing with the short coil. A comparison of ϕ_M and what I call $\phi_F = R_s/R_{ac}$ is given in Table 6. The Fraga formula was evaluated for 18 gauge wire at 1 MHz to make it as comparable as possible to the Medhurst experiment.

Table 6: Comparison of ϕ_M with ϕ_F for a coil with $\ell_w/D = \infty$

d/z_1	ϕ_M	ϕ_F
1.0	3.41	3.19
0.9	3.11	3.03
0.8	2.81	2.86
0.7	2.51	2.67
0.6	2.22	2.48
0.5	1.93	2.26
0.4	1.65	2.03
0.3	1.40	1.75

We see that the Fraga formula agrees best with Medhurst for a wire diameter to wire spacing ratio of between 0.8 and 0.9, which happens to be the typical ratio for tight wound magnet wire. Therefore, there is hope for the Fraga formula for typical Tesla coils (tight wound magnet wire with a length/diameter ratio of at least four).

I then proceeded to compare the coil resistance R_s predicted by Fraga with the coil resistance R_M predicted by Medhurst and with the measured resistance R_{TC} for my coils. Results are given in Table 7.

This table gives the wire diameter $d = 2b$ in both mils and mm, the coil radius a, the winding length ℓ_w, the total length of wire used in the coil, the number of turns N, the Wheeler inductance L, the Medhurst capacitance C_M, the Medhurst factor ϕ_M interpolated from Table 3, and the dc resistance R_{dc} at 20^oC. Measured inductance is always close to the calculated value from Wheeler's formula. Measured resistance agreed with the calculated value to within 1% or so, when corrected for temperature.

Table 7: Predicted and Measured Coil Resistance for Several Coils

	12T	14S	14T	16B	18B	18T	20T	22T	22B
$2b$, mils	80.81	64.08	64.08	50.82	40.30	40.30	31.96	25.35	25.35
$2b$, mm	2.053	1.628	1.628	1.291	1.024	1.024	.8118	.6439	.6439
a, meters	.231	.198	.107	.24	.235	.107	.107	.107	.24
ℓ_w, meters	1.613	1.166	1.392	.7	.47	.881	.952	.945	.7
wire, meters	509	482	623	675	617	534	702	424	675
turns N	351	387	797	445	418	794	1052	631	445
L, mH	14.2	17.2	19.34	49.4	55.02	29.1	47.3	17.2	49.4
C_M, pF	30.58	23.95	20.70	22.66	21.22	15.45	16.14	16.08	22.66
ϕ_M	1.68	1.85	3.03	4.20	4.25	3.15	3.02	1.62	1.54
R_{dc}	2.66	3.99	4.45	8.89	12.9	11.2	23.4	22.4	35.7
f_0, kHz	246.4	247.6	251	153.5	147.3	236.9	181.1	301.5	153.5
R_s	22.83	29.99	44.11	51.13	62.49	67.55	97.33	65.94	69.00
R_M	17.96	24.7	46.35	80.93	95.61	76.50	111.39	58.38	66.09
R_{TC}	18.7	24.5	43.5	93.1	118.0	70.5	94.2	47.0	73.0
f		217.3	211.3	128.4	123.6	176.1	135.9	227.9	129.5
R_s		28.10	40.48	46.76	54.04	58.23	84.47	56.76	62.23
R_M		23.13	41.67	74.97	88.92	66.52	98.37	51.57	55.00
R_{TC}		25.6	42.3	87.1	103.0	65.9	88.0	46.7	69.5
f		158.8	151.8	91.9	86.2	122.5	94.2	158.1	93.1
R_s		24.02	34.31	39.56	46.90	48.57	70.40	45.76	51.74
R_M		20.06	35.86	64.76	76.65	57.03	85.04	44.56	55.00
R_{TC}		24.5	39.6	75.0	78.9	58.1	78.7	42.4	66.8

The suffix S refers to space wound, while T refers to a tight wound coil. The suffix B refers to a barrel whose sides are not perfectly straight, for coils 16B and 22B. The winding is tight wound on the flat portions of the barrel and space wound on the transition portions. The barrels were assumed to be made of polyethylene when I purchased them at the local recycling plant. The barrels used for 12T and 18B are straight sided and have thinner walls than the 16B and 22B barrels. They were once used as tanks for water softeners. Coil 14S is on a coil form built from a 0.125 inch sheet of polyethylene. Coils 14T, 18T, 20T, and 22T are on PVC forms. Coil 20T has 3 layers of polyurethane on it, the others have no coating. Coil 12T is made in two sections for ease of handling.

The 12 ga wire is Essex type USE-2 (or type RHH or type RHW-2), which are types specified in the National Electrical Code. This type has a relatively thick insulation, which spaces the conductors farther apart than the thin insulation of magnet wire. It has a nominal insulation thickness of 45 mils as compared to a 15 mil thickness for the more common Type THHN. The 14, 16, 18, and 20 ga wires are magnet wires coated with Heavy Soderon. This

Essex coating has a top layer of nylon. Magnet wires are available with one, two, three, and four layers of insulation. Heavy Soderon is equivalent to a two layer coating. The 22 gauge wire is not magnet wire but has a yellow insulating jacket, that I assume is PVC. The wire was acquired surplus and the numbers are difficult to trace.

The Medhurst capacitance and the Wheeler inductance are used to calculate the resonant frequency f_0. The actual resonant frequency was measured with a HP54645 digital scope. Agreement was within 5%. The operating resonant frequency will always be lower than the unloaded value due to the toroid on top, so this number is of mostly academic interest anyhow.

The observed resistances include displacement current effects and any dielectric losses, which might increase the actual resistance well above that due to copper losses alone. The highest frequency in the table refers to the case of no top load, while lower frequencies were obtained with different sizes of toroids mounted on top the coil.

Coil 14T has the greatest length/diameter ratio (6.47) of the group, so we would expect Fraga's formula to work the best for this case. Indeed, it predicts a resistance only about 4% less than that predicted by Medhurst, both close to the experimental values.

As we move to coil 18B, which has the smallest length/diameter ratio (1.0), Fraga's formula significantly under predicts the resistance, being about 55% of observed and about 63% of the Medhurst values.

On the other hand, coil 22T has a reasonable length/diameter ratio (4.42), but greater dielectric thickness s, and Fraga's formula over predicts the resistance, being about 124% of observed and about 109% of Medhurst.

For the seven coils 14T–22B, Fraga's formula predicts resistance values about 90% of what Medhurst predicts. All things considered, this is pretty good. If we stick with coils close wound with magnet wire, and a length/diameter ratio of 4 or more, Fraga's formula should be quite acceptable.

The next step was to determine the character of the transition of resistance values as frequency is raised from dc to those frequencies where the proximity effect is fully implimented. That is, there is no proximity effect at dc. The measured resistance of a coil is the same as the same length of straight wire. As frequency increases, however, the skin effect causes resistance to increase, and the proximity effect causes resistance to increase even more. Presumeably, at a high enough frequency where the skin depth is a small fraction of the wire radius, the proximity effect saturates. The measured resistance continues to increase, but only due to the skin effect.

I measured the input resistance as a function of frequency for seven of my coils, 14T, 16B, 18B, 18T, 20T, 22T, and 22B. This includes all five coils with a Medhurst factor $\phi_M = R_{TC}/R_{ac}$ of 3.0 or more. I used a standard bench function generator with sine wave output, followed by a linear amplifier. The amplifier is a simple single-stage inverting op-amp, using the Apex PA-19, rated at 4 A, ±36 V, slew rate 900 V/μs. Voltage was measured with a standard scope probe, current with a Philips PM9355 current probe. The output of the current probe was fed to the second channel of the scope, a HP54645D digital oscilloscope capable of calculating rms values of measured waveforms. I applied a voltage between about 2.5 and 10 V (rms) to the base of the coil, tuned the function generator for resonance, observed the current value, and calculated the resistance as the ratio of voltage to current.

The test location was inside a 54 by 90 ft metal building (manufactured by Morton) that is typically used for livestock or storage of ag equipment. One 15 by 30 ft corner was framed in, insulated, and equipped with furnace and air conditioner. Inside this instrument room was a double copper wall Faraday cage with footprint 8 by 12 ft. Electricity was provided to this screen room through an isolation transformer and power line filters. The computer, oscilloscope, and other sensitive equipment were located in this screen room. It is interesting to note that reception on a transistor AM radio was not affected by moving it from outside to inside the Morton building, but reception was impossible inside the screen room, even with the massive copper door open. The AM band starts at 550 kHz, slightly above most of my testing in the 100–300 kHz range, so it would appear that the Faraday cage was effective in the necessary frequency range. I never observed any failures in electronic equipment inside the cage that I could link to transient high fields outside the cage.

This Morton building has a wood frame and wood trusses supporting the roof. There is no ceiling so the wood trusses and roof are visible inside the building. The bottoms of the trusses are about 16 ft above the floor. Depending on the location, the roof will be about 17 to 25 ft above the floor.

Except for the screen room, all electrical outlets in the building were wired in the conventional manner for North America, with the third wire connected to utility ground. This ground wire is connected to earth at every power pole on the utility system. I installed my own ground system under the dirt floor of the Morton building, consisting of three lengths of copper tubing buried a foot or so below floor level. The soil is very hydrophilic, so when I water the grass on the outside of the building, the copper tubing is located in wet earth. The measured resistance between this local ground and utility system ground was on the order of 1 Ω, a quite acceptable value. Open circuit voltage between the two grounds may be as high as several volts, and current flow between grounds may be as high as several amps. The utility ground is a major source of noise in sensitive measurements, so all measurements were made using only the local ground. The Faraday cage was connected to this local ground, as well as the metal skin of the Morton building.

A damp earth floor made the interior of the building too humid, so I covered the floor with polyethylene sheets, and covered those with about four inches of milled asphalt. This is a product obtained when asphalt roads are recycled. If carefully packed, it forms almost as nice a surface as concrete, and is much less expensive. It is also much easier to penetrate if one wanted to install something in the earth.

Even though the local ground is very satisfactory for making sparks with Tesla coils, I was concerned that variations in earth moisture would affect my proximity effect measurements. I therefore installed a metal ground plane on top of the asphalt millings, about 8 by 16 ft, consisting of sheets of aluminum siding bonded together with copper flashing and sheet metal screws. This would obviously not be suitable for spark tests when hundreds of kV and tens of amps are present, but for low level measurements of a few volts and less than one amp should be ok.

The coil under test was placed on a piece of 2 inch thick blue styrofoam on this metal ground plane. Location was about 10 ft from the wall of the Morton building and about 10 ft from the wall of the instrument room. A length of 50 Ω coaxial cable was run under the ground plane, through the wall of the instrument room, through the wall of the Faraday cage, and to the function generator. The shield of the coax was connected to the ground plane close to the base of the coil. The center conductor of the coax was connected to the base of the coil, so the coil was driven like a vertical helix above a ground plane. With no toroid or other connection to the top of the coil, the inductance of the coil would resonate with the Medhurst capacitance. This would be the maximum frequency at which the impedance could be measured.

Capacitance could be increased and frequency lowered by placing larger and larger toroids on top the coil. However, it is not feasible to have toroids large enough to lower the frequency to a few kHz, as required for this test. Different size toroids also change the local field distribution, which might affect the results. So I decided to connect a capacitor to the top of the coil, and the other lead of the capacitor to a heavy ground wire that went up from the top of the coil to about 10 ft above the floor, over to the wall of the instrument room, and down to the floor where it was connected to both the metal ground plane and to the copper tubing of the local ground. Electrically, this forms a simple series RLC circuit. If large value capacitors are used, the resonant frequency can be under 1 kHz.

Like many other things about Tesla coils, using the wrong type of capacitor can lead to surprises. The voltage rating is important, as a little thought will reveal. The Q of these coils is high, perhaps as high as 500. Driving the coil with 10 V would then put as much as 5000 V across the capacitor. My first effort was to use variable capacitors here. I had a ham type variable capacitor that would handle the voltage, but receiving type variable capacitors would arc over between the plates. Even when the voltage was acceptable, the resistance of the sliding contacts in the capacitors was too high (and too erratic) at the required current levels.

The final solution was to place an aluminum cake pan, flat bottom up, on top of the coil and electrically connected to it. A half spun aluminum toroid was connected to the hanging ground wire. Polyethylene sheets were placed on the cake pan and the half spun toroid would be placed on the sheets, flat side down, to form a simple parallel-plate capacitor. Different thicknesses would allow for the resonant frequency to be lowered to about one fourth of the maximum value. For even lower frequencies, lumped capacitors were used.

Figure 3 shows the variation of R_{TC}/R_{ac} versus frequency for the coil 14T, plotted solid with diamond symbols. It also shows the Fraga resistance R_s divided by R_{ac}, plotted dashed. Theory and experiment match extremely well. Again, the Fraga formula works well for long coils that are tight wound with magnet wire.

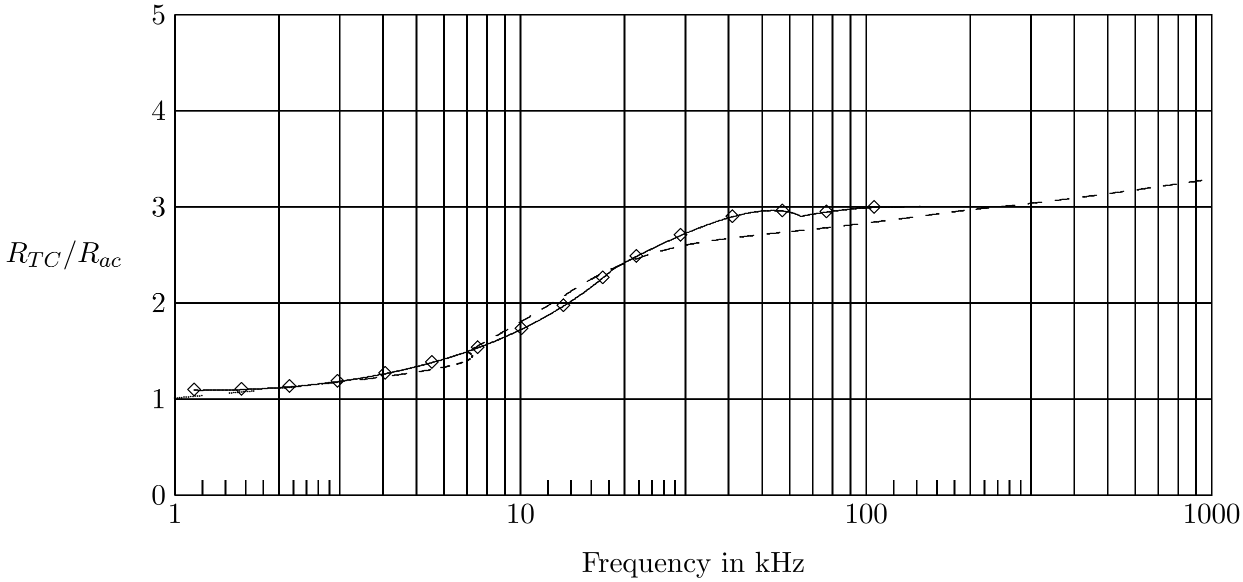

Figure 3: R_{TC}/R_{ac} for coil 14T

I then performed the same measurements of R_{TC} for coil 18B, the shortest coil in my collection. Results are shown in Fig. 4. The Medhurst ϕ_M is 4.25 for this coil where ϕ_F is about 3. The predictions by Fraga are below the measured values over the entire range of frequencies. Even worse, the experimental and theoretical start to diverge at about 50 kHz.

I have performed other tests which show that this particular magnet wire absorbs moisture, and this moisture will cause increased losses. Dielectric losses are entirely separate from the proximity effect. It appears that the dielectric losses become significant above 50 kHz for coil 18B, causing the ratio R_{TC}/R_{ac} to go well above the value ϕ_M predicted by Medhurst for the case with negligible dielectric losses.

Figs. 3 and 4 also show another effect, a very interesting concept that is otherwise difficult to explain. This concept is that there is little penalty in performance if one uses a smaller wire in a coil. That is, the effect on spark length is not as strongly related to the wire resistance as one would expect.

If one looks closely at these figures, it is evident that the transition region moves higher in frequency as the wire gets smaller. At a given frequency, the larger wire will always be closer to saturation. Consider an extreme example where two coils are each wound with 1000 ft of magnet wire, one with 14 ga and the other with 28 ga. Assume the coils are resonant at 70 kHz and that $\phi_M = 3$. The dc resistance of the 14 ga coil is 2.525 Ω while the dc resistance of the 28 ga coil is 64.9 Ω, a factor of 25.7 greater. The ac resistances at 70 kHz are, from Eqs. 30 or 32, (1.888)(2.525) = 4.768 Ω for the 14 ga coil and (1.0034)(64.9) = 65.1 Ω for the 28 ga coil. The 14 ga coil has reached full saturation from the proximity effect at 70 kHz, so

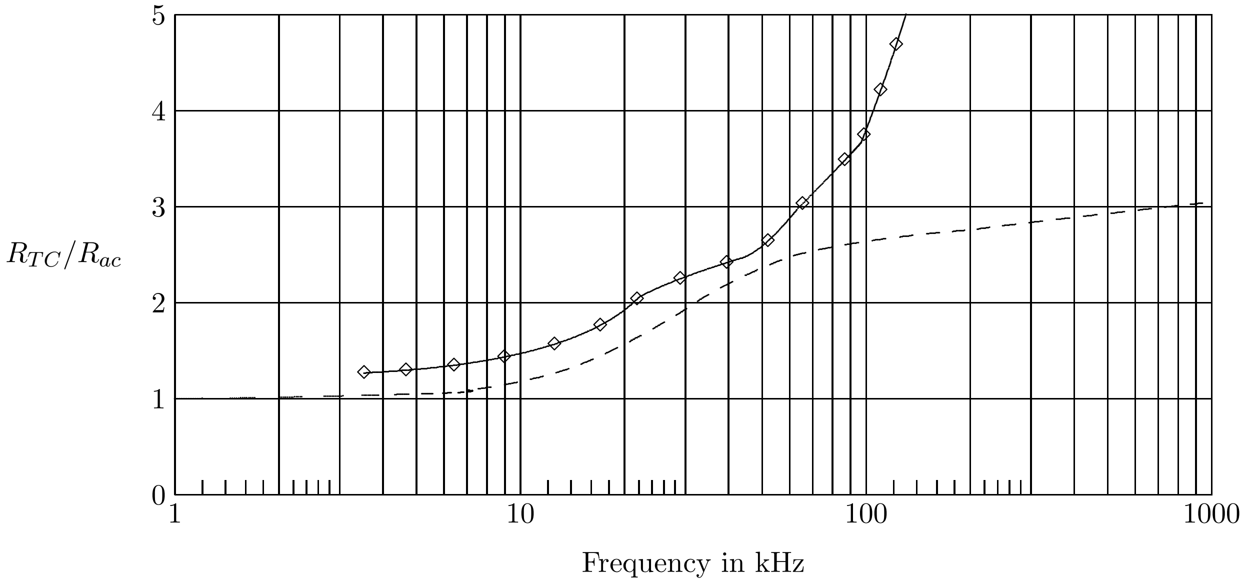

Figure 4: R_{TC}/R_{ac} for coil 18B

the effective R_{TC} is (4.768)(3) = 14.3 Ω. The 28 ga coil has not started into the proximity effect yet at 70 kHz, so its resistance is still just 65.1 Ω. The ratio of resistances at 70 kHz is 65.1/14.3 = 4.55, a considerable reduction from 25.7.

It would have been nice to finish this treatment of copper losses with a formula that was accurate to within 5% for any frequency, any length/diameter ratio, and any wire diameter to wire spacing ratio. But that remains for someone else. I hopefully have described the problem so that the reader can get within perhaps 20% of the correct value, and sometimes even better.

4 Displacement Current Effect

We have examined two methods for empirically or theoretically determining the copper loss in a coil, the methods of Medhurst [5] and Fraga [2]. These both assume that the conduction current is the same at all points in the coil, which is the usual case for circuit theory type RLC models. But this is not necessarily the case for a Tesla coil. This is one place where the lumped circuit models just cannot go. We finally have to use a distributed approach. If the conduction current is less than the input current in part of the coil, we would expect the effective resistance to also be less. Likewise, if the conduction current is greater than the input current, then we would expect the effective resistance to increase. Conduction current can be greater than the input current in one part of a coil, and less in another part, due to displacement currents. We will try to illustrate this concept with Fig. 5. A Tesla coil is connected to a toroid with a switch S_1. The input current at the base is the conduction current i_{in}.

Every part of the coil has a capacitance to every other part. We show four capacitors in this four turn coil, C_{21} from turn 2 to turn 1, C_{42} from turn 4 to turn 2, C_{t2} from the toroid to turn 2, and C_{2g} from turn 2 to ground. Each capacitor has a current flow in it, with the same subscripts.

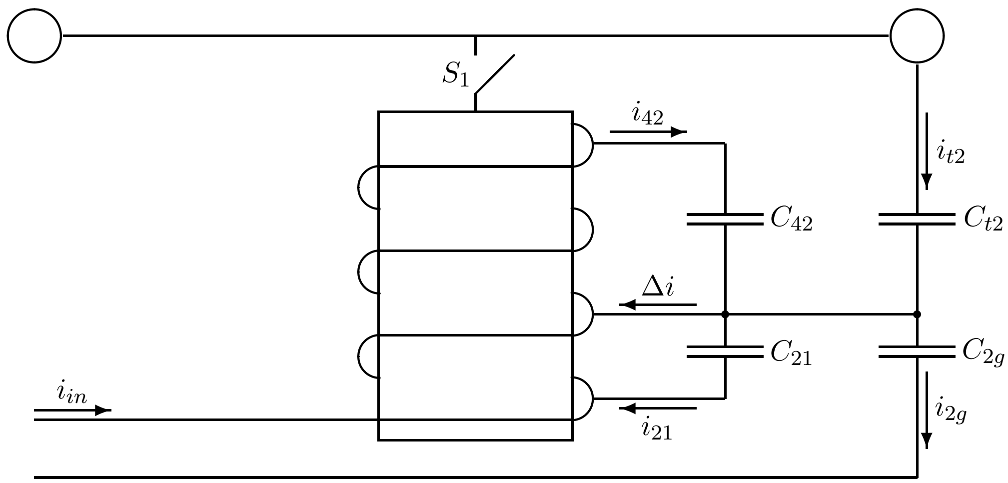

Figure 5: Conduction Current

The incremental current entering turn 2 is

$$\Delta i = i_{42} + i_{t2} - i_{21} - i_{2g} \tag{60}$$

If the two currents i_{42} and i_{t2} are greater than the other two currents, then Δi is positive. If the current in turn 1 is i_{in} and Δi is added in turn 2, then the current in turn 3 is greater than i_{in}. This situation is quite possible for the lower part of the coil where many turns above the turn in question are adding currents and only a few turns below are subtracting currents. It is more likely to occur if C_{2g} is small, that is, if the coil is mounted well above a ground plane.

On the other hand, as we get toward the top of the coil, there are many turns below the turn in question that are subtracting currents from Δi and only a few turns above that are adding currents. The minimum current occurs in the top turn of the coil. If switch S_1 is open (no toroid), this minimum current is zero. So we have the situation where the current increases in the lower part of the coil, will hit a maximum probably somewhere in the middle third of the coil, and then start to decrease toward the minimum current value at the top of the coil.

Possible variations of conduction current in the coil winding as a function of position y is shown in Fig. 6. The current marked "S_1 closed" is a possible current with toroid while the current marked "S_1 open" is a possible current without a toroid.

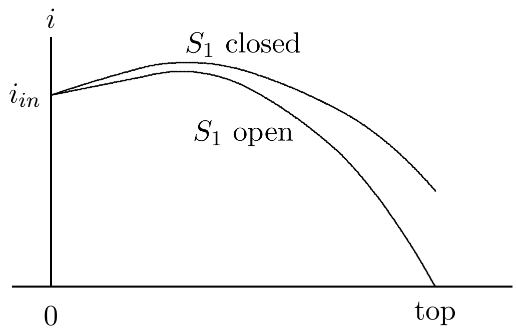

Figure 6: Conduction Current in a Coil

There are several qualitative factors that can be deduced from these curves, without going to the effort to do the full distributed analysis. We started on this quest by asking "Is the lumped RLC model for the Tesla coil a useful concept, or must we proceed immediately to the distributed model?" If this distributed effect is not too big, such that any fudge factor is no more than a few percent, then we can still use the lumped model. If the effect is too big, then we will be inclined to use the distributed model in order to get decent results.

We note that the current in the coil is greater than the input current in the lower part of the coil and less over the upper part of the coil. These tend to offset each other so that the effective resistance may not be much different from the resistance calculated for the uniform current case.

As larger toroids are added, the current in the coil increases, and likewise the effective resistance. However, the resonant frequency decreases with larger toroids, which lowers the effective resistance for the uniform current case. This predicts a smaller change in resistance with frequency than predicted by either Medhurst or Fraga.

The final qualitative factor is that if a coil has a geometry that causes the peak current in the coil to be well above the input current (say 30% or more), the effective resistance will also be well above that for the uniform current case. We can now go back to Table 7 and check out these predictions.

We note that for coil 14T, the measured resistance is *below* both R_s and R_M for a coil without a toroid and *above* both R_s and R_M for a coil with the largest toroid. The measured resistance holds more nearly constant with variation in frequency than is predicted by Medhurst or Fraga, a very consistent observation throughout all my testing.

It appears that as coils get shorter and fatter, the interior current in the coil gets larger and the effective resistance increases as compared with the predictions of Medhurst and Fraga. Consider coils 22T and 22B. Coil 22T (relatively long and thin) has a measured resistance below the predictions, while coil 22B (short and fat) has a measured resistance above the predictions. The other two short coils (16B and 18B) also have measured resistances above the predictions.

The average ratio of R_{TC} over R_s for the coils 14T, 18T, 20T, and 22T was 1.004, while the average ratio of R_{TC} over R_M for these four coils was 0.927. It appears to me that for normal Tesla coil geometries (length/diameter = 4 or more) that the uniform current assumption is not too bad. It appears to yield accuracies within ±10%, which should be acceptable in most applications. We conclude that the displacement current effect is very real and easily observed in data sets like Table 7, but the errors involved in ignoring it are not so severe that we cannot use the lumped model.

5 Dielectric Losses

We turn now to losses in the coil form and in the wire insulation. Both the coil form and the wire insulation form a part of the coil capacitance. By Gauss's Law the coil capacitance is the sum of electric flux lines leaving the coil, divided by the coil voltage. Some flux lines go from toroid to earth through the coil form, some from turn to turn through the wire insulation, and some through air. These can be considered as three capacitors in parallel. Since the volumes of the coil form and the wire insulation are much smaller than the volume of air, and the relative permittivity is only two or three times that of air, their capacitances will be a small part of the total. The losses may still be significant, of course.

If we assume a linear increase of voltage along the coil, the flux lines in the coil form will be uniform from top to bottom (no fringing) just like the parallel plate capacitor. We should be able to use the formula for the parallel plate capacitor without great error.

Dielectric losses are usually modeled by a resistor in parallel with the capacitance, rather than in series. They are related to the capacitor voltage rather than to the capacitor current. We have two dielectrics, the coil form and the wire insulation, so we have two resistors in parallel with the Tesla coil capacitance. We saw equations for the power dissipation in the coil form, P_{cf}, and in the wire insulation, P_{wi}, back in Chapter 3. If the toroid voltage is V_{tor}, then the parallel resistances can be defined as

$$R_{cf} = \frac{V_{tor}^2}{P_{cf}} \tag{61}$$

$$R_{wi} = \frac{V_{tor}^2}{P_{wi}} \tag{62}$$

A somewhat more detailed RLC model is shown in Fig. 7. The resistances directly related to current are shown as R_M, R_{eddy}, R_{spark}, and R_{rad}, where the last three items are the equivalent resistances representing losses to eddy currents in toroid and ground plane, the spark itself (when present), and any losses due to radiation. We considered the Medhurst resistance R_M earlier in the chapter. You can replace R_M by R_s from Fraga's formula if you prefer. The resistances related to voltage are R_{cf} and R_{wi}.

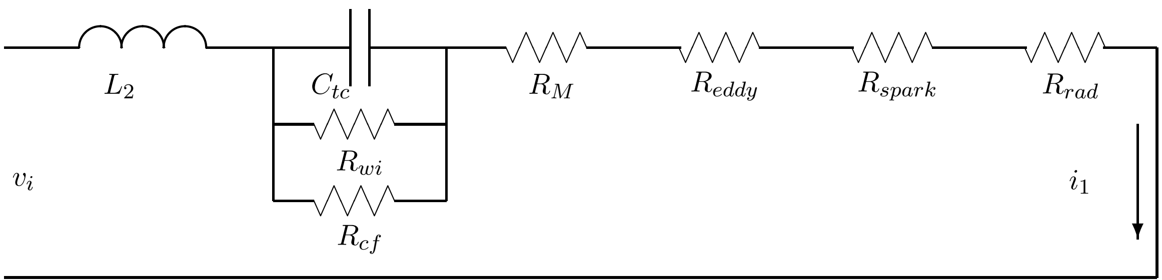

Figure 7: Detailed Lumped Model of Tesla Coil

For single-frequency, steady-state operation, the parallel combination of a capacitor and two resistors can be modeled as a series capacitor and resistor, call it R_{die}. This is straightforward Circuit Theory I, but a bit tedious. We write an expression for the parallel impedance of R_{cf}, R_{wi}, and the capacitance, rationalize it, and simplify the real term. We assume that the parallel resistances are much larger than the capacitive reactance, as they will be for any coil with acceptable losses. The algebra goes as follows:

$$Z = \frac{1}{1/R_{wi} + 1/R_{cf} + j\omega C_{tc}} = \frac{1}{G + j\omega C_{tc}} = \frac{G - j\omega C_{tc}}{(G + j\omega C_{tc})(G - j\omega C_{tc})} \tag{63}$$

We define R_{die} as the real part of Z.

$$R_{die} = \text{Real } Z = \text{Real}\left(\frac{G - j\omega C_{tc}}{G^2 + \omega^2 C_{tc}^2}\right) \approx \frac{G}{\omega^2 C_{tc}^2} = \frac{P_{cf} + P_{wi}}{V_{tor}^2 \omega^2 C_{tc}^2} \tag{64}$$

To make things even more complicated, we will define R_{die} as the series combination of three resistors, the series coil form resistance R_{cfs}, the series wire insulation resistance R_{wis1}, and the series coating resistance R_{wis2}. If there is no coating on the coil (polyurethane or equivalent) and if the wire and atmosphere are dry then $R_{wis2} = 0$.

$$R_{die} = R_{cfs} + R_{wis1} + R_{wis2} \tag{65}$$

The revised circuit model for the Tesla coil is shown in Fig. 8.

We now proceed to get specific equations for these three series resistors, referring back to Chapter 3 for the power dissipated in terms of V_{tor}.

$$R_{cfs} = \frac{P_{cf}}{V_{tor}^2 \omega^2 C_{tc}^2} = \frac{V_{tor}^2 \omega C_{cf} (DF)_{cf}}{V_{tor}^2 \omega^2 C_{tc}^2} = \frac{C_{cf}(DF)_{cf}}{\omega C_{tc}^2} \tag{66}$$

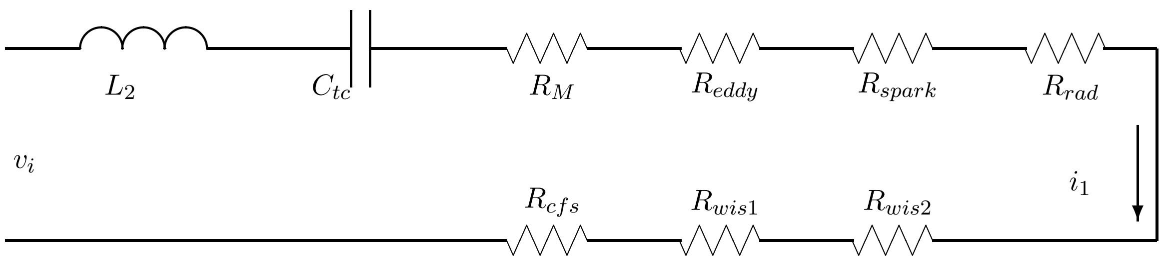

Figure 8: Lumped Model of Tesla Coil with Series R_{die}

$$R_{wis1} = \frac{\epsilon_2^2(\eta_o - \eta_x)(\pi\epsilon_1\ell_t)(DF)_1}{N\omega C_{tc}^2[\eta_o\epsilon_2 + \eta_x(\epsilon_1 - \epsilon_2)]^2} \tag{67}$$

$$R_{wis2} = \frac{\epsilon_1^2\eta_x(\pi\epsilon_2\ell_t)(DF)_2}{N\omega C_{tc}^2[\eta_o\epsilon_2 + \eta_x(\epsilon_1 - \epsilon_2)]^2} \tag{68}$$

It would appear that R_{die} *decreases* as $1/\omega$ or as $1/f$. This is certainly contrary to our intuition. What is even more surprising is that the dissipation factor of water is also proportional to $1/\omega$ over the typical Tesla coil frequency range. $(DF)_{\text{water}} = 0.396$ at $f = 10^5$ Hz and 0.0396 at $f = 10^6$ Hz [3]. This would make R_{die} vary as $1/\omega^2$. I have not convinced myself that this is correct, but can see no flaw in the above analysis. I will terminate the theoretical discussion of dielectric losses on that note.

There are many things going on that make it difficult to be precise about frequency variation of the other losses, but generally speaking, R_{ac} increases as $\sqrt{f}$, and R_{eddy} increases as f^2. R_{rad} will increase at a rate somewhere between f and f^2. R_{spark} can be ignored below the spark inception voltage. Depending on which terms are dominant loss terms, we may not see a pronounced change in input impedance with frequency. That has been my experience. Input impedance will drift from day to day, (mostly with humidity), but there is no obvious frequency dependence. Of course, other things are happening. We know that R_{ac} increases with temperature, while R_{die} increases with humidity. If these were the only factors, we would expect a cold, dry winter day to have the lowest impedance, and a hot, muggy day to have the highest impedance and the worst performance. In cases where moisture is a factor, performance might improve after a period of operation which caused the coil form to heat up and dry out.

Moisture has been a very frustrating factor in my testing. Coils are located inside a metal skin building with no climate control, in eastern Kansas. Temperatures can vary from below freezing to 40^{o}C (104^{o}F) or more. Relative humidities vary from 25% to 100%. Typical of my measurement problems are two sets of input impedance data in Table 8 for 3/17/01 and 4/6/01. The 3/17/01 data were collected when the bay temperature was about 9^{o}C and the relative humidity was about 28%. On 4/6/01 the temperature was about 17^{o}C and the relative humidity was 100%. It had been damp all week with heavy fog the day before.

Table 8: R_{TC} Measured on Two Different Days

Coil	14S	14T	16B	18T	18B	20T	22T	22B
frequency, kHz	249.1	266.1	145.5	242.6	145.6	183.6	307.0	148.3
R_{TC} 3/17/01	24.5	43.5	93.1	70.5		94.2	47.0	73.0
R_{TC} 4/6/01	27.6	45.5	175.8	75.7	127.7	100.0	53.4	126.7

We see that two of the coils experienced large changes in R_{TC}, coils 16B and 22B. Both coils used a plastic barrel as a coil form that I thought was polyethylene. I got the barrels at the local recycling plant. Coil 22B used the same type of wire as coil 22T which was wound on a piece of PVC, so the difference in R_{TC} between these two coils had to be the coil form. These results indicate that some coil forms are worse than others. These barrels evidently soak up water in amounts sufficient to raise the input impedance by a factor of two.

Coils 14T, 18T, 20T, and 22T were wound on PVC while coils 14S and 18B were wound on polyethylene. Only coil 20T had any type of coating put on top the winding (polyurethane). Both PVC and polyethylene appear to have about the same increase in R_{TC} with humidity, so it is hard to argue that one should spend more money on the more expensive polyethylene.

As long as one stays with good quality coil forms, it appears that high humidity will raise R_{TC} by 5–10% from the low humidity case. One could reverse engineer Eq. 67 and find an effective dissipation factor $(DF)_1$ that would be an appropriate function of humidity, but I am not sure it would be worth the trouble.

The eddy current loss will be a strong function of how near the conducting material is located to the coil. A coil sitting on a ground plane would have a much larger R_{eddy} than one sitting on a one meter high stack of Styrofoam blocks. If soil moisture affects the eddy current loss in the earth beneath the coil, then this term could vary widely from day to day. If tests are being done inside a metal building, then the walls and roof of the building would contribute to the eddy current loss.

Many coils have a strike ring located around their base, to intercept sparks before hitting the feed line or other components. There is general agreement in the Tesla coil community that this ring should be open rather than shorted. There have been observations where a shorted copper ring has significantly degraded spark length. A spun aluminum toroid also presents a shorted path for eddy currents, but there is less agreement that this represents a significant loss. It is argued that conduction currents are smaller at the top of the coil, therefore induced currents must be less.

I built a toroid of 0.25 inch copper tubing pieces on insulating disks, connected together at one point by a conducting disk. The ends were placed into heat shrink tubing, which was then shrunk to hold the ends a fixed small distance apart. This toroid was then compared with a spun aluminum toroid of similar capacitance, and also with a smaller toroid made of one inch copper tubing with diameter slightly greater than that of the coil form. The smaller toroid was an attempt to get a shorted turn as near to the coil as possible. It lacked the capacitance to be an effective toroid for long sparks, of course. I could not find any significant difference in input impedance between the insulated toroid and the spun aluminum toroid. The shorted copper ring, however, had about 10% higher input impedance than the toroid that was not a shorted turn. This suggests that you would not notice any improvement if you cut your beautiful spun aluminum toroid into pieces to eliminate eddy currents. The effect is there, and can be measured if one really works at it, but is not that significant in most situations.

Overall, my tests indicated that R_{eddy} is no more than a few percent of R_{TC}. If a little thought is given to separation of conducting materials from the immediate vicinity of the coil, eddy current losses can be ignored. Likewise in all my tests, R_{rad} is very close to zero. I was unable to detect a signal from the coil more than perhaps 100 m away. At worst, it would be a number like 0.01 Ω, which is a negligible portion of a typical measured resistance of 25 to 50 Ω.

6 Conclusion

I believe that Fig. 8 is a reasonable model for a Tesla coil. There is scientific basis for calculating (or estimating) R_M, R_{cfs}, R_{wis1}, and R_{wis2}, and for ignoring R_{eddy} and R_{rad}. It has the proper indication for changes in the model when a spark occurs. The model indicates that when a spark occurs, the equivalent resistance R_{spark} increases from zero to some finite value, so the input resistance *increases* during a spark. This is exactly what happens experimentally.

Unfortunately, great precision is difficult to impossible to obtain. R_M or R_s can be calculated to within a few ohms given the techniques in this chapter. I consider this a vast improvement over my state of knowledge when I started this project. Trying to get more accuracy is probably not warranted because of the strong influence of moisture on coil resistance. If R_M is $50 \pm 5\Omega$, and R_{die} might vary from 0 to 5 Ω or more as humidity goes from 0 to 100%, there is little point in reducing the uncertainty on R_M.

In my opinion, a complete distributed model will not be any better in dealing with skin effect, proximity effect, and dielectric losses, and would certainly be more of a programming problem. The one thing that this lumped model cannot deal with directly is the displacement current effect. A distributed model can determine the actual current distribution, which can then be used to find a predicted effective resistance of the coil.

Both approaches (lumped and distributed) have advantages. I believe the lumped approach is better at determining resistance. However, the lumped approach will not show anything about resonances at harmonic frequencies, and cannot deal with things like the current distribution. Hopefully there will be peaceful coexistence, where each method will be used to its full advantage.

References

[1] Benson, Barry, bensonbd@erols.com, Private communication, November, 2001.

[2] Fraga, E., C. Prados, and D.-X. Chen, "Practical Model and Calculation of AC Resistance of Long Solenoids", *IEEE Transactions on Magnetics*, Vol. 34, No. 1, January, 1998, pp. 205–212.

[3] Harrington, R. F., *Time–Harmonic Electromagnetic Fields*, McGraw–Hill, New York, 1961. p.455

[4] Jahnke, Eugene and Fritz Emde, *Tables of Functions*, Dover, 1945.

[5] Medhurst, R. G., "H.F. Resistance and Self-Capacitance of Single-Layer Solenoids", *Wireless Engineer*, February, 1947, pp. 35-43, and March, 1947, pp. 80-92.

[6] Ramo, Simon, John R. Whinnery, and Theodore Van Duzer, *Fields and Waves in Communication Electronics*, Second Edition, John Wiley, 1984.

[7] Smythe, William R., *Static and Dynamic Electricity*, Hemisphere Publishing Corporation, A member of the Taylor & Francis Group, New York, Third Edition, Revised Printing, 1989.

[8] Terman, Frederick Emmons, *Radio Engineers Handbook*, McGraw-Hill, 1943.